Z. Phys. B – Condensed Matter 83, 143–151 (1991)

Condensed
Zeitschrift für Physik B Matter

Dispersive optical bistability in a nonideal Fabry-Pérot cavity

II. Numerical results on side-mode instabilities

A.J. van Wonderen and L.G. Suttorp

Institute for Theoretical Physics, Valckenierstraat 65, 1018 XE Amsterdam, The Netherlands

Received August 1, 1990

Instabilities in the nearest side-modes are predicted for dispersive optical bistability in a nonideal Fabry-Pérot cavity. Our results are based on a linear stability analysis of the Maxwell-Bloch equations. This analysis leads to a boundary value problem for a four-dimensional set of linear differential equations, which we have solved numerically. Our findings show that the instability spectrum strongly depends on the detuning parameters and on the transmission coefficient of the cavity mirrors. If the atomic detuning gradually increases, instability domains are found to merge. If moreover the cavity detuning grows, instabilities spread along the upper branch of the bistability curve, even for high values of the medium response time. We have made a comparison between our results and recent experimental data, the outcome of which is satisfactory from a qualitative point of view. Finally, we show that the side-mode instabilities for dispersive optical bistability in a Fabry-Pérot cavity are incorrectly predicted, if a so-called equivalent ring cavity is adopted as a model.

1. Introduction

In an accompanying paper [1], hereafter referred to as I, we have performed a linear stability analysis of the Maxwell-Bloch equations for dispersive optical bistability in a Fabry-Pérot cavity with mirrors of finite transmission coefficient. On the basis of this theory one can make predictions on instabilities in passive media with feedback. These instabilities may destroy a stationary state of the system in such a way that it evolves to a state in which the transmitted intensity undergoes spontaneous sinusoidal pulsations, at a fixed value of the input intensity.

The self-pulsing phenomenon in a passive medium is driven by beats between the signal from the external laser beam and a signal that is generated by the medium enclosed in the cavity. The frequency of the latter signal is determined by the cavity modes and the atomic transition. Amongst the cavity modes the mode of which the frequency lies closest to that of the external laser signal is called the resonant mode. If this mode is the only one involved in building up the instability the latter is said to be of the single-mode type. In the other case, that is to say, if off-resonant cavity modes are excited as well, the instability is of the multimode or side-mode type. In this treatment we shall focus on multimode instabilities which are caused by a spontaneous excitation of the nearest side-modes, i.e. the off-resonant cavity modes that lie nearest to the resonant mode on the frequency axis. Such instabilities are characterized by a self-pulsing frequency of the same order of magnitude as the free spectral range of the cavity.

Recently [2, 3], a self-pulsing behaviour has been observed in a passive medium of two-level molecules. In the experimental setup the optical cavity was of the Fabry-Pérot type. The medium was neither in resonance with the laser beam nor with the resonant cavity mode. On the basis of arguments that were put forward some time ago for a ring cavity [4] the experimental observations were interpreted as being generated by instabilities in the nearest side-modes. In the present treatment, in which both dispersive and standing-wave effects are fully taken into account, we shall be able to test this interpretation.

In Sect. 2 we shall formulate our stability problem in such a way that it can be solved numerically. In Sect. 3 we shall discuss the problems that may arise in exploring the parameter space of our model. Actual results are presented in Sect. 4. Our numerical search for instabilities starts from the purely absorptive case and gradually shifts to the parts of the parameter space that were covered in the experiment. Besides a comparison with the experimental data we also make a comparison with the theoretical predictions for the case of a so-called equivalent ring cavity [2].

2. Formulation of the stability problem

As we have shown in I a linear stability analysis of the Maxwell-Bloch equations for dispersive optical bistabil-

ity in a Fabry-Pérot cavity leads to the following set of linear differential equations

$$\frac{\mathrm{d}}{\mathrm{d}\zeta}\begin{pmatrix}\Delta^{(+)}f\\ \Delta^{(+)}b\\ \Delta^{(-)}f\\ \Delta^{(-)}b\end{pmatrix}=\begin{pmatrix}H_{11} & H_{12} & H_{13} & H_{14}\\ H_{21} & H_{22} & H_{23} & H_{24}\\ H_{31} & H_{32} & H_{33} & H_{34}\\ H_{41} & H_{42} & H_{43} & H_{44}\end{pmatrix}\begin{pmatrix}\Delta^{(+)}f\\ \Delta^{(+)}b\\ \Delta^{(-)}f\\ \Delta^{(-)}b\end{pmatrix}. \tag{2.1}$$

The quantities $\Delta^{(+)}f$ and $\Delta^{(-)}f$ are the amplitude deviation and the phase deviation of the forward electric field, respectively, while the quantities $\Delta^{(+)}b$ and $\Delta^{(-)}b$ denote the amplitude and the phase deviations of the backward electric field. The matrix elements H_{ij} depend on the eigenvalue λ of the stability probem and on the stationary forward and backward fields f and b, which in their turn are a function of the spatial variable $\zeta=z/L$, with L the length of the cavity. The explicit form of the matrix H has been given in I.

The spatial behaviour of the deviations of the electric fields is completely determined by the differential Eq. (2.1) and a boundary condition at $\zeta=1$, which we derived in I. It reads

$$\begin{pmatrix}\Delta^{(\pm)}f(1)\\ \Delta^{(\pm)}b(1)\end{pmatrix}=\tfrac{1}{2}\Delta^{(\pm)}x\begin{pmatrix}1\\ R^{1/2}\end{pmatrix}, \tag{2.2}$$

where R is the reflection coefficient of the cavity mirrors. Hence, each electric field deviation is given by a linear combination of the amplitude deviation $\Delta^{(+)}x$ and the phase deviation $\Delta^{(-)}x$ of the output envelope x. The coefficients of these combinations depend on the spatial coordinate ζ. For $\zeta=0$ we can formally write

$$\begin{pmatrix}\Delta^{(+)}f(0)\\ \Delta^{(+)}b(0)\\ \Delta^{(-)}f(0)\\ \Delta^{(-)}b(0)\end{pmatrix}=\begin{pmatrix}\mathscr{A}\\ \mathscr{B}\\ \mathscr{C}\\ \mathscr{D}\end{pmatrix}\Delta^{(+)}x+\begin{pmatrix}\mathscr{E}\\ \mathscr{F}\\ \mathscr{G}\\ \mathscr{H}\end{pmatrix}\Delta^{(-)}x. \tag{2.3}$$

The mirrors of the cavity impose a condition on the deviations of the electric fields at $\zeta=0$. This condition, which can be found in I, reads

$$\begin{pmatrix}\Delta^{(+)}f(0)\\ \Delta^{(-)}f(0)\end{pmatrix}=R^{1/2}\begin{pmatrix}\cos\alpha & \sin\alpha\\ -\sin\alpha & \cos\alpha\end{pmatrix}\begin{pmatrix}\Delta^{(+)}b(0)\\ \Delta^{(-)}b(0)\end{pmatrix}, \tag{2.4}$$

with $\alpha=\Delta\log|b(0)/(f(0)R^{1/2})|-\theta$. In this last expression the so-called detuning parameters of our model figure. The atomic detuning Δ is the scaled difference between the atomic frequency ω_a and the laser frequency ω, that is $\Delta=(\omega_a-\omega)/\gamma_\perp$, with $\gamma_\perp$ the transverse damping coefficient of the medium. The symbol $\gamma_\parallel$ denotes its longitudinal counterpart. The cavity detuning θ accounts for the fact that in general the laser is not in perfect resonance with the cavity. It is defined according to $\theta=2L(\omega-\omega_n)/c$, with $\{\omega_n\}$ the cavity frequencies. On the frequency axis these are separated from each other by a distance $\pi c/L$, the free spectral range.

Substituting (2.3) into (2.4) we obtain a set of two linear equations for $\Delta^{(+)}x$ and $\Delta^{(-)}x$. These equations have a nonzero solution, if the determinant of the associated matrix vanishes. In this way we arrive at the condition

$$\begin{vmatrix}\mathscr{A}-\mathscr{B}R^{1/2}\cos\alpha-\mathscr{D}R^{1/2}\sin\alpha & \mathscr{E}-\mathscr{F}R^{1/2}\cos\alpha-\mathscr{H}R^{1/2}\sin\alpha\\ \mathscr{C}-\mathscr{D}R^{1/2}\cos\alpha+\mathscr{B}R^{1/2}\sin\alpha & \mathscr{G}-\mathscr{H}R^{1/2}\cos\alpha+\mathscr{F}R^{1/2}\sin\alpha\end{vmatrix}=0. \tag{2.5}$$

If we consider (2.1)–(2.5) for the purely absorptive case and accordingly set the detuning parameters equal to zero, we find that (2.1) separates into two independent sets of equations, one for the amplitude deviations and one for the phase deviations. As a consequence, the quantities $\mathscr{C}$, $\mathscr{D}$, $\mathscr{E}$ and $\mathscr{F}$ vanish. Since $\alpha=0$ for the absorptive case, the condition (2.5) factorizes into two separate conditions as well. Hence, for perfect resonance between the laser, the cavity and the medium the linear stability analysis of the Maxwell-Bloch equations gives rise to two decoupled stability problems, one for the amplitudes and another for the phases of the field envelopes.

The vectors at the right-hand side of (2.3) depend on the eigenvalue λ and on the parameters of our model. Therefore, the determinant at the left-hand side of (2.5) can be seen as a function Ψ of these quantities, at least in a formal way. The dependence of λ on the system parameters follows from the condition that the function Ψ must equal zero. It is interesting to notice that the only complex quantity in the stability problem is the eigenvalue λ. This implies the equality $\Psi^*(\lambda)=\Psi(\lambda^*)$, so that the set of solutions of the stability problem is invariant under the operation $\lambda\to\lambda^*$. Furthermore, each solution λ is invariant under the transformation $(\Delta,\theta)\to(-\Delta,-\theta)$.

In the above we used the qualification 'formal' for the reason that actual computation of the function Ψ is out of the question. We must solve the stability problem numerically. To that end, a numerical integration of the set (2.1) has to be performed. Because of the fact that the matrix H depends on the spatial variable ζ via the stationary electric fields f and b, it is convenient to choose instead of ζ a combination χ of these fields, namely

$$\chi=2|f'|^2+2|b'|^2+2K-\tfrac{1}{2}, \tag{2.6}$$

with the definition

$$4K=-|x'|^2(1+R)+[T^2|x'|^4+2|x'|^2(1+R)+1]^{1/2}, \tag{2.7}$$

where T stands for $1-R$. We used the abbreviation $v'=v(1+\Delta^2)^{-1/2}$, with $v=f$, b and x. From the stationary theory discussed in I it follows that the matrix H can directly be written in terms of the new variable χ via the relations

$$4|f'|^2=\chi+\tfrac{1}{2}-2K+(\chi^2-\tfrac{1}{2}+2K)^{1/2}, \tag{2.8}$$

$$4|b'|^2=\chi+\tfrac{1}{2}-2K-(\chi^2-\tfrac{1}{2}+2K)^{1/2}. \tag{2.9}$$

To transform the left-hand side of (2.1) one must use

$$\frac{d\chi}{d\zeta}=-C'T\frac{(\chi^2-\frac{1}{2}+2K)^{1/2}}{\chi+\frac{1}{2}}, \tag{2.10}$$

with $C'=C(1+\Delta^2)^{-1}$ the scaled cooperation parameter of optical bistability. This parameter is defined as $C=\alpha L/T$, with α the absorption coefficient of the medium. Finally, we need to specify the interval of integration on the χ-axis. The condition (2.2) must hold at $\chi=\chi_1 \equiv\frac{1}{2}|x'|^2(1+R)-\frac{1}{2}+2K$, while (2.5) is to be imposed at $\chi=\chi_0$, with χ_0 determined by the equality

$$[(\chi_0^2-\tfrac{1}{2}+2K)^{1/2}+\chi_0]\exp(2(\chi_0^2-\tfrac{1}{2}+2K)^{1/2}]$$
$$=(|x'|^2-\tfrac{1}{2}+2K)\exp(2C'T+T|x'|^2), \tag{2.11}$$

as follows from (2.29)–(2.31) of I.

The integration of the set (2.1), in which the expressions for the matrix elements H_{ij} have to be inserted, is reduced now to a purely numerical problem. To solve it we have employed integration routines of the Merson and of the Adams type [5]. As an initial condition for the integration one has to use (2.2). If we choose the vector $(\Delta^{(+)}x, \Delta^{(-)}x)$ equal to (1, 0) and integrate towards χ_0 we obtain the quantities $\mathscr{A}$ to $\mathscr{D}$ from the electric field deviations; the choice (0, 1) provides us with the quantities $\mathscr{E}$ to $\mathscr{H}$. Subsequently, we can determine λ such that the constraint (2.5) is satisfied by employing a root-finding program. In this way solutions for the eigenvalue λ are found as functions of the parameters of the system.

Before discussing the numerical results it is useful to investigate the stability problem of the Maxwell-Bloch equations for a few special cases so that we get an idea of the analytical structure of the stability problem and of the kind of solutions for λ that can be expected. This will help in interpreting the numerical solutions for the general case.

3. Analytic structure of the stability problem

The stability problem as formulated in the previous section consists of a set of linear differential equations with boundary conditions which together determine the eigenvalue λ. A stationary solution of the Maxwell-Bloch equations becomes unstable for some specific values of the parameters, if any of the eigenvalues λ acquires a positive real part. In order to find the parameter values for which this happens one needs to follow the evolution of all eigenvalues, at least in principle. If one is only interested in multimode instabilities caused by the nearest side modes, as we are in this paper, it is sufficient to consider those eigenvalues of which the imaginary parts are of the order of the free spectral range of the cavity. Even then it is not an easy task to ascertain whether all relevant eigenvalues have been taken into account. As it turns out the analysis of the eigenvalue problem for the particular case of nearly ideal mirrors, i.e. mirrors with small transmission coefficient, can be of great help here. In that case, which corresponds to the uniform-field limit [6], the solution of the stability problem can be obtained in analytic form. For absorptive optical bistability in a Fabry-Pérot cavity the uniform-field theory has been employed before [7].

To illustrate the use of the uniform-field limit we shall first consider a simple stability problem, namely that of purely absorptive optical bistability in a folded ring cavity of length $2L$. The stability problem [6] falls apart into two separate problems, one for the amplitude deviations and one for the phase deviations. We shall discuss them both, starting with the latter.

The differential equation that governs the phase deviations reads

$$\frac{d}{d\zeta}\Delta^{(-)}f=-2\tilde{\lambda}\Delta^{(-)}f-\frac{CT}{\lambda_\perp(1+4f^2)}\Delta^{(-)}f, \tag{3.1}$$

with $\zeta=z/(2L)$ and $\tilde{\lambda}=\lambda L/c$. Furthermore, $\lambda_\perp$ stands for $1+\gamma_\perp^{-1}\lambda$, while C is the cooperation parameter $2\alpha L/T$ in the present case. The stationary field $f(\zeta)$ satisfies the relation

$$\log\left[\frac{f(\zeta)}{f(1)}\right]+2[f^2(\zeta)-f^2(1)]=CT(1-\zeta), \tag{3.2}$$

with $f(1)$ given by the amplitude $|x|$ of the outgoing field through the boundary condition $f(1)=|x|/2$. The differential Eq. (3.1) can easily be solved by introducing $4f^2$ as a new integration variable. One finds

$$\Delta^{(-)}f(\zeta)=\Delta^{(-)}f(1)\exp\left[2\tilde{\lambda}(1-\zeta)+\frac{1}{2\lambda_\perp}\int_{4f^2(1)}^{4f^2(\zeta)}\frac{ds}{s}\right]. \tag{3.3}$$

Imposing the boundary condition $\Delta^{(-)}f(0)=R\Delta^{(-)}f(1)$ we arrive at a quadratic equation for λ the solution of which is

$$2\tau_\perp\tilde{\lambda}=\sigma\tau_\perp-1\pm\left[(\sigma\tau_\perp+1)^2-2\tau_\perp\log\left(\frac{f(0)}{f(1)}\right)\right]^{1/2}. \tag{3.4}$$

Here we abbreviated $\tau_\perp=c/(L\gamma_\perp)$ and $\sigma=\pi n\mathrm{i}+\frac{1}{2}\log R$, for integer n. For each n the stability problem has yielded two solutions, which differ only by the sign in front of the complex square root function.

The fact that the stability problem has got two independent solutions for each n can be inferred already from a study of the uniform-field limit of (3.3). In that limit $f(0)$ and $f(1)$ are nearly equal. Consequently, the integration interval shrinks to zero. The contribution of the integral thus becomes small provided the factor $(2\lambda_\perp)^{-1}$ in front of the integral remains finite. If this condition is satisfied one recovers the well-known uniform-field solution for this problem

$$\tilde{\lambda}=\pi n\mathrm{i}+\mathcal{O}(T). \tag{3.5}$$

On the other hand, if the factor $(2\lambda_\perp)^{-1}$ is of the order of T^{-1} the contribution of the integral in (3.3) remains

finite. The solution then gets the form

$$\tilde{\lambda} = -\tau_{\perp}^{-1} + \mathcal{O}(T). \tag{3.6}$$

In first order of T both solutions depend on the cavity mode index n. Of course, they can be derived from (3.4) as well. However, the point we wish to stress is that the existence of additional solutions of the type (3.6) can be demonstrated already on the basis of (3.3) by studying the behaviour of the integral in the uniform-field limit.

Obviously, the solution (3.6) does not give rise to instabilities in the uniform-field limit. Deviations governed by this solution decay on a time scale given by the polarization relaxation time $\gamma_{\perp}^{-1}$ and may hence be called 'relaxation solutions'. One should realize however, that on moving away from the uniform-field régime it is not obvious a priori that these relaxation solutions remain as harmless as they have started. Yet, by using the explicit expression (3.4) one can prove that they do not give rise to instabilities for any T.

Turning to the stability problem for the amplitude deviations we can perform a similar analysis. These deviations are determined by the differential equation

$$\frac{\mathrm{d}}{\mathrm{d}\zeta} \Delta^{(+)} f = -2\tilde{\lambda} \Delta^{(+)} f + \frac{CT(4f^2 - \lambda_{\parallel})}{(1+4f^2)(\lambda_p + 4f^2)} \Delta^{(+)} f, \tag{3.7}$$

where $\lambda_{\parallel} = 1 + \gamma_{\parallel}^{-1} \lambda$ and $\lambda_p = \lambda_{\parallel} \lambda_{\perp}$. Introducing the new variable $4f^2$, as before, we obtain the solution in the form

$$\Delta^{(+)} f(\zeta) = \Delta^{(+)} f(1) \exp\left[2\tilde{\lambda}(1-\zeta) + \tfrac{1}{2} \int_{4f^2(1)}^{4f^2(\zeta)} \mathrm{d}s \frac{\lambda_{\parallel} - s}{s(\lambda_p + s)} \right]. \tag{3.8}$$

This solution has to be supplemented by the boundary condition $\Delta^{(+)} f(0) = R \Delta^{(+)} f(1)$. Carrying out the integral we end up with a transcendental equation for λ. We shall not pursue that line any further. Instead, we directly turn to a consideration of the uniform-field limit, as before. In that limit the integral in (3.8) will generally yield a contribution proportional to T, since the integration interval is of order T. Consequently, the eigenvalues $\tilde{\lambda}$ that satisfy the boundary condition again have the form of (3.5). However, this conclusion is incorrect if the factor $\lambda_p + s$ in the integrand becomes of order T for $s = 4f^2(1) = |x|^2$. In that case the eigenvalue $\lambda^{(0)}$ in leading order of T follows from the quadratic equation

$$(\lambda^{(0)} + \gamma_{\perp})(\lambda^{(0)} + \gamma_{\parallel}) + \gamma_{\perp} \gamma_{\parallel} |x|^2 = 0. \tag{3.9}$$

The amplitude instability problem thus leads to two 'relaxation solutions', which both have a negative real part. If T moves away from zero it is not an easy matter to ascertain whether these relaxation solutions are going to give rise to instabilities.

As demonstrated above the occurrence of relaxation solutions in the uniform-field limit could be assessed by studying the integral representations (3.3) or (3.8). The explicit solutions of the differential equations were not needed. We can go a step further by remarking that even the integral representations need not to be written down. The differential equations (3.1) and (3.7) themselves are already sufficient to draw conclusions about the existence of relaxation solutions in the uniform-field limit, since the presence of this type of solutions is a direct consequence of the fact that the coefficients of $\Delta^{(+)} f$ and $\Delta^{(-)} f$ may blow up for a suitable choice of λ.

Armed with this knowledge we now reconsider the stability problem given in the previous section. To determine whether relaxation solutions will be present we have to look for possible singularities in the coefficients H_{ij} that occur in the set of differential equations (2.1). Upon inspection of the explicit expressions as given in I it follows that relaxation solutions will indeed show up. Some of these are found by choosing the eigenvalue $\lambda^{(0)}$ in leading order to T in such a way that one of the factors $\lambda_{\perp}$ or $1 + \Delta^2/\lambda_{\perp}^2$, which occur in the denominators of the matrix elements H_{ij}, vanishes. For small T the ensuing relaxation solutions have the form

$$\lambda^{(0)} = -\gamma_{\perp}, \qquad \lambda^{(0)} = \gamma_{\perp}(-1 \pm \mathrm{i}\Delta). \tag{3.10}$$

Other relaxation solutions follow by putting the factor W_{λ} occurring in H_{ij} equal to zero. In the uniform-field limit it reduces to

$$U_{\lambda} = \left[1 + 4 \frac{|x|^2}{\lambda_p (1 + \Delta_{\lambda}^2)} \right]^{1/2}. \tag{3.11}$$

In leading order of T the corresponding solutions thus follow from the cubic equation

$$[(\lambda^{(0)} + \gamma_{\perp})^2 + \gamma_{\perp}^2 \Delta^2](\lambda^{(0)} + \gamma_{\parallel}) + 4\gamma_{\perp} \gamma_{\parallel} (\lambda^{(0)} + \gamma_{\perp}) |x|^2 = 0. \tag{3.12}$$

We have now found six relaxation solutions, which are present on a par with the standard uniform-field solutions that have been discussed in I. Similar solutions have been derived for the ring cavity [6]. None of the solutions given by (3.10) and (3.12) have a positive real part, so that in the uniform-field limit these relaxation solutions do not lead to unstable behaviour. However, it remains to be seen whether this conclusion still holds if T is increased.

Up to now we have tacitly assumed that the various solutions for λ can be treated separately. However, it can be seen already from (3.4) this this is an illusion. The two solutions given there are related since both contain the same double-valued complex square-root function. If the argument of that function encircles the origin of the complex plane the two solutions get interchanged. A similar phenomenon can happen for the more complicated stability problem associated with dispersive optical bistability in a Fabry-Pérot cavity. In fact, a square-root function already occurs in the uniform-field expression for the eigenvalue λ, which reads according to I

$$\tilde{\lambda} = \pi n \mathrm{i} + \tfrac{1}{2} T[\alpha \pm (\alpha^2 - 4\beta)^{1/2}], \tag{3.13}$$

up to first order in T. The quantities α and β are complex; they depend on the system parameters and the integer n, which specifies the cavity mode. Clearly, one can no longer distinguish between the two solutions when the

argument of the square-root function moves through the complex plane.

The above considerations make clear that one should be careful in performing a numerical analysis of the stability problem for dispersive optical bistability in a nonideal Fabry-Pérot cavity. In principle, it cannot be excluded that the solutions which are the continuations of the relaxation solutions towards finite T will eventually lead to unstable behaviour for some T. As it is virtually impossible to follow the evolution of all solutions as the system parameters are gradually changed we have adopted the following strategy in our numerical work. We have started from the purely absorptive case and have determined the behaviour of the eigenvalue solutions for vanishing medium response times $\tau_i = c/(L\gamma_i)$ with $i = \perp, \parallel$. In this so-called adiabatic régime transients in the medium die out instantaneously, so that relaxation solutions cannot play a role. Subsequently, we have studied the continuations of these adiabatic solutions for finite values of τ_i and of the detuning parameters Δ and θ. As a next step we have checked our results by following the evolution of the uniform-field solutions for the dispersive case as T grows to a finite value. In this way we hope to obtain a fairly complete picture of the solutions λ that may give rise to unstable behaviour.

4. Side-mode instabilities

In this section we present our results on side-mode instabilities for dispersive optical bistability in a nonideal Fabry-Pérot cavity. These have been obtained by a numerical analysis of the mathematical problem formulated in Sect. 2. As remarked in the previous section a full analysis of the stability problem is difficult to realize, since in principle one should follow all solutions for all values of the system parameters. As stated above, we have limited ourselves to an analysis of the solutions that are obtained by a continuation of the absorptive adiabatic solutions towards finite $\tau_\perp$, $\tau_\parallel$, Δ and θ, and of the dispersive uniform-field solutions towards finite T. Even with this limitation the exploration of all parts of parameter space is a tremendous task, as there are seven independent parameters specifying the system (viz. T, C, Δ, θ, $|x|$, $\tau_\perp$ and $d \equiv \gamma_\parallel/\gamma_\perp$). In choosing T, C, Δ, θ and d we have mainly focused on values for which experimental results are available [2]. In particular, we have put d equal to unity throughout. Keeping these parameters fixed we have located the regions in the parameter space where the system is unstable by calculating the curves in the $(|x|, \tau_\perp)$-plane for which the real parts of the eigenvalues equal zero.

As a starting-point of our numerical treatment we have set both detuning parameters Δ and θ equal to zero so that the optical bistability is purely absorptive. The instability problem then falls apart into an amplitude and a phase problem. Furthermore, we have chosen the cooperation parameter C equal to 300. For a vanishing medium response time $\tau_\perp$, which corresponds to the adiabatic régime, we have raised the mirror transmission coefficient T from 0 to 0.05 and followed the two nearest-side-mode solutions for λ, with Im $\lambda L/c$ of the order of π. Subsequently, we have scanned both solutions for increasing $\tau_\perp$. In this way, we have encountered two instability domains for the amplitude problem and one for the phase problem. All three are directly connected with the standard uniform-field solutions if T is lowered to zero. The domains have been drawn in Fig. 1. For the purely absorptive case we have already discussed the behaviour of these domains as a function of the system parameters in earlier papers [9]. Now we want to investigate how they change if we enter the dispersive régime.

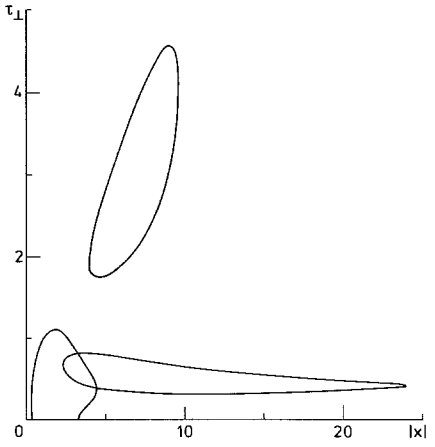

Fig. 1. Instability domains of the nearest side-modes in the $(|x|, \tau_\perp)$-plane for the purely absorptive case $\Delta = \theta = 0$, with $T = 0.05$ and $C = 300$. The long domain parallel to the $|x|$-axis is generated by the phase stability problem, the other two domains by the amplitude problem

To analyze the dispersive stability problem we have studied how the instability domains of Fig. 1 are influenced upon increasing Δ, still keeping $\theta = 0$, $C = 300$ and $T = 0.05$. In drawing instability domains in the $(|x|, \tau_\perp)$-plane for a fixed finite Δ one should take notice of the fact that small $\tau_\perp$-values correspond to large differences between the atomic and the laser frequencies. As such large differences are unphysical we introduce a new detuning parameter $\tilde{\Delta} = \Delta/\tau_\perp$. At a fixed value for $\tilde{\Delta}$ the adiabatic limit $\tau_\perp \to 0$ is no longer of academic interest only. In fact, for $\theta = 0$ it gives rise to the same stability problem as for the absorptive adiabatic case.

If we increase the atomic detuning $\tilde{\Delta}$ to a finite value while keeping $\theta = 0$ and $T = 0.05$, the domain near the $|x|$-axis in Fig. 1, which we have called the adiabatic domain in our earlier work [9], slightly shrinks. This tendency is seen up to $\tilde{\Delta}$-values of the order of unity. More interesting is the behaviour of the other two domains in Fig. 1. At increasing $\tilde{\Delta}$ both these domains approach each other and for $\tilde{\Delta}$ near 0.3 they merge. This may come as a surprise, as these domains have evolved from two separate stability problems at $\tilde{\Delta} = 0$, each with its own eigenvalue solution. The paradox is solved by returning to the observation made in the previous section in connexion with (3.13). Eigenvalues of the dispersive problem may become many-valued functions owing to the coupling of two instability problems that were

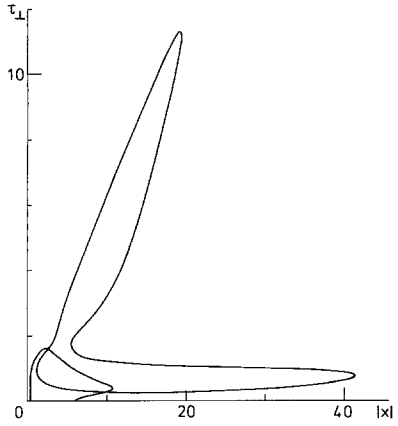

Fig. 2. Instability domains of the nearest side-modes in the $(|x|, \tau_\perp)$-plane for $\tilde{\Delta}=0.2$, $\theta=0$, $T=0.1$ and $C=300$

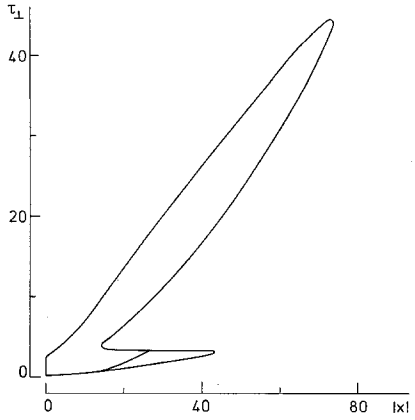

Fig. 3. Dispersive instability domain for the nearest side-modes at $\tilde{\Delta}=1$, $\theta=0$, $T=0.31$ and $C=294$. The line cutting through the domain marks the onset of upper-branch instabilities

uncoupled in the absorptive case. Indeed, this many-valued character of the eigenvalue has been checked numerically by following its evolution along a suitably chosen closed path in the $(\tilde{\Delta}, \tau_\perp)$-plane. It turns out that the eigenvalue is a two-valued function which returns to its original value only when the closed path is followed twice in succession.

Upon repeating the above analysis for higher values of T we have found that roughly the same phenomena happen as described for $T=0.05$. The adiabatic domain does not move appreciably, while the other two instability regions join forces. The situation for $T=0.1$ and $\tilde{\Delta}=0.2$ is shown in Fig. 2. From the shape of the big domain, to be called the dispersive domain from now on, one can clearly see that it has been generated by a fusion of two domains. The adiabatic domain and the dispersive domain partly overlap; they correspond to different solutions for λ at $\tilde{\Delta}=0.2$. With regard to Fig. 2 it is also of interest to remark that the influence of the transmission coefficient T on the stability of the nearest side-modes has changed completely by going from the absorptive to the dispersive régime. In the former case the instability domains tend to contract towards low values of $\tau_\perp$, if T increases [9]. In contrast, in the dispersive case with $\tilde{\Delta}=0.2$ instabilities are present up to $\tau_\perp = \mathcal{O}(10)$ both for $T=0$ and $T=0.1$.

We have made sure that this tendency of the system to be unstable at rather large values of $\tau_\perp$ persists if $\tilde{\Delta}$ and T are increased still further. In Fig. 3 the dispersive domain has been drawn for $\tilde{\Delta}=1$ and $T=0.31$, at $C=294$. These values are of interest in view of experimental results that we shall discuss below. The instability region given in Fig. 3 causes unstable behaviour up to $\tau_\perp=44.6$. (It should be noticed that the scales of Figs. 1–3 are different.) We have not plotted the adiabatic domain in Fig. 3. It is contained in the box defined by $0.24 \leqq |x| \leqq 24$ and $0 \leqq \tau_\perp \leqq 1.8$, so that it is much smaller than the dispersive domain.

Not all parts of the instability domains are of equal physical importance. Most interesting is that part of the domains that corresponds to instabilities along the upper branch of the curve describing the stationary behaviour.

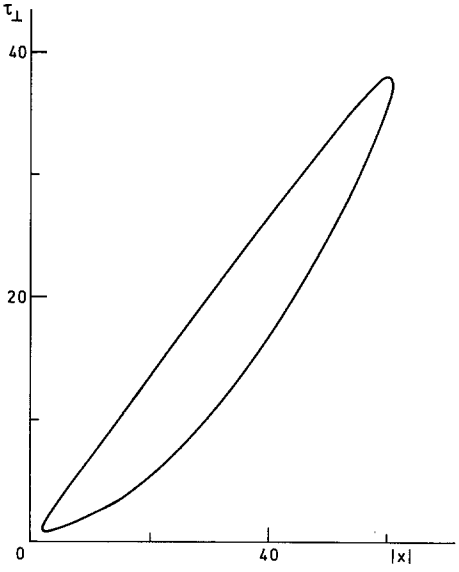

Fig. 4. Instability domain of the nearest side-modes as predicted by uniform-field theory for $\tilde{\Delta}=1$, $\theta=0$ and $C=294$

In Fig. 3 this part is situated to the right of the line that divides the lower portion of the domain. Hence, the major part of the domain does not give rise to instabilities in the upper branch.

As a check on the results described so far we have followed an alternative route to investigate the instability domains of dispersive optical bistability, namely by starting from uniform-field theory corresponding to $T=0$. The influence of increasing detuning parameters on the instability domains can conveniently be studied in the framework of this theory as well. In the purely absorptive case, with Δ and θ both equal to zero, the uniform-field theory predicts that at $C=294$ instabilities are only found in the box given by $2.6 \leqq |x| \leqq 10.4$ and $0.94 \leqq \tau_\perp \leqq 4.9$. If we increase $\tilde{\Delta}$ the uniform-field instabilities spread to parts of the $(|x|, \tau_\perp)$-plane outside this box. For $\tilde{\Delta}=1$ the uniform-field domain has been plotted in Fig. 4. The domain has grown considerably in going

from $\tilde{\Delta}=0$ to $\tilde{\Delta}=1$. If we compare the domain of Fig. 4 with the dispersive domain of Fig. 3, which pertains to $T=0.31$, we see that at $\tilde{\Delta}=1$ the instabilities encountered in uniform-field theory do not gradually disappear for increasing T. Earlier [9], we have established that for $\tilde{\Delta}=0$ they do. This observation on the behaviour of instabilities in the dispersive case confirms the statement we made in our comment on Fig. 2.

To demonstrate the link between the domains of Figs. 3 and 4 we have calculated the boundaries of the uniform-field domain at $\tau_\perp=16.5$ for various values of T from 0.01 till 0.31. It turns out that differences with the uniform-field prediction are less than one percent throughout. Of course, the imaginary part of $\tilde{\lambda}$ does not stay close to π for increasing T. It takes values between 3.05 and 3.43. Uniform-field theory thus performs excellently, even for $T=0.31$, at least if $\tau_\perp$ equals 16.5. The last qualification is essential: for low values of $\tau_\perp$ the uniform-field predictions fail at high T. For instance, the characteristic bend in the dispersive domain of Fig. 3 is not predicted by uniform-field theory.

We have now discussed how the instability domains drawn in Fig. 1 evolve if both Δ and T increase. Our main conclusion is that two of these domains merge and that the resulting domain gradually extends towards rather high values of $\tau_\perp$, when $\tilde{\Delta}$ gets of the order of unity. Whereas the instability domains never reach the range $\tau_\perp=\mathcal{O}(10)$ for the absorptive case [9], they easily attain $\tau_\perp$-values as high as 30 for $\tilde{\Delta}=1$. These findings are quite interesting in view of the interpretation of recent experimental results the discussion of which we now turn our attention to.

The experiment which has been carried out at the University of Lille [2, 3] was devised to observe self-pulsing behaviour of the multimode type in a passive medium of molecules that effectively behaved as two-level particles. The optical cavity in the experiment was of the Fabry-Pérot type, with an effective mirror reflection coefficient $R=0.69$ and with a stunning length of 182 meters. This configuration permits the observation of instabilities in the nearest side-modes. The experimental cooperation parameter was $C=294$, while the damping coefficients $\gamma_\perp$, $\gamma_\parallel$ of the medium were approximately equal. The atomic detuning and the cavity detuning could both be varied in the experiment.

In comparing the experimental findings with those of the present treatment it should be kept in mind that in our theory the mirrors are supposed to be free from internal absorption so that we could write $T=1-R$. On the other hand, in the experiment there is no simple relation between T and R. However, what really matters in our theory is the value of R, since the reflection coefficient controls the internal feedback in the system. The transmission coefficient T of the mirrors enters the formalism only through the coefficients of the amplitudes of the incoming and the outgoing electric fields that figure in the boundary conditions. Since in the experiments these fields are determined up to an unspecified scale factor the precise value of T will be of no concern. Hence, in comparing our results with those of the experiments we have to replace T in our theory by $1-R$ and take

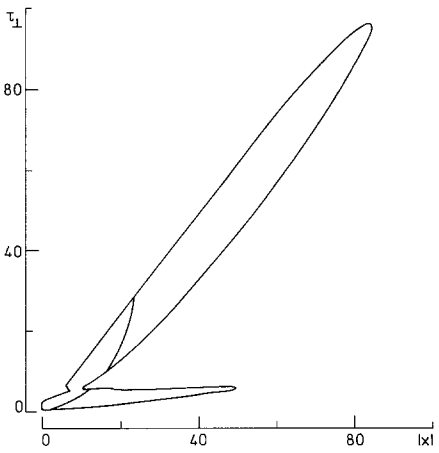

Fig. 5. Dispersive instability domain for $\tilde{\Delta}=1.21$, $\theta=-2.42$, $T=0.31$ and $C=294$. The lines cutting through the domain mark the onset of upper-branch instabilities

R equal to the effective reflection coefficient 0.69 of the mirrors used in the experiment. As to the detuning parameters $\tilde{\Delta}$ and θ, we shall make free use of the invariance of our theory under the transformation $(\tilde{\Delta}, \theta)\rightarrow(-\tilde{\Delta}, -\theta)$.

In Fig. 10 of [2] an example of an experimental bistability curve has been shown. It has been obtained by slowly varying the input intensity $|y|^2$ at $\tau_\perp=21.8$, $\Delta=1.21$ and $\theta=-2.42$. The experimental curve exhibits a pronounced self-pulsing phenomenon in its upper branch. This self-pulsing of the output intensity has been attributed to an instability in the nearest side-modes. If this is the case it makes sense to try and reproduce its features on the basis of the theoretical description of steady-state optical bistability and of the instability domains as given in I and in the present paper. In Fig. 5 the dispersive instability domain is shown for optical bistability under the experimental conditions. If we compare it with the dispersive domain of Fig. 3 we see that the decrease of θ from zero to -2.42 is responsible for a growth of the domain in the $\tau_\perp$ direction by a factor 2. Furthermore, the peculiar constriction of the domain near $\tau_\perp=6$ is more pronounced in Fig. 5. As in Fig. 3 we have drawn lines through the domain beyond which positive-slope instabilities are present. It can be seen from Fig. 5 that instabilities may be present along a considerable part of the upper branch of the bistability curve, if $\tau_\perp<6$. Moreover, in contrast to the findings of Fig. 3 for which $\theta=0$, upper-branch instabilities extend towards rather high values of the medium response time. The actual experimental value for $\tau_\perp$ is 21.8. For this value of the medium response time instabilities are present in the interval $|x|\in[18.1, 30.0]$ according to our findings. Computation of the eigenvalue $\tilde{\lambda}$ for increasing $|x|$ in this interval shows that Re $\tilde{\lambda}$ attains a maximum value of 0.105 at $|x|=24.5$, while Im $\tilde{\lambda}$ steadily increases from 2.33 to 2.55 at $|x|=29.3$ and decreases beyond the latter value.

In Fig. 6 the steady-state curve for the experimental circumstances of Fig. 10 of [2] is presented. If one suitably multiplies the scales $|x|^2$ and $|y|^2$ the curve covers

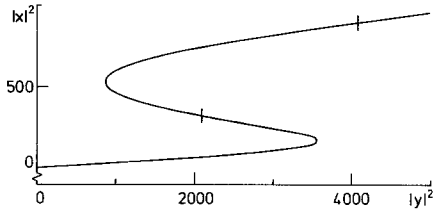

Fig. 6. Steady-state curve for $\Delta=26.4$, $\theta=-2.42$, $T=0.31$ and $C=294$. The part between vertical dashes is unstable

the experimental bistability curve in a satisfactory way. The ratios r of the $|y|^2$-values for the turning points as obtained from the theoretical and the experimental curves differ by 10%. The vertical dashes crossing the curve of Fig. 6 indicate the boundaries of its unstable part as predicted by the dispersive domain of Fig. 5 for $\tau_\perp=21.8$. Clearly, the region of instabilities extends over a substantial part of the upper branch of the bistability curve, as found in the experiment. The imaginary part of $\tilde{\lambda}$ can be used as an estimate for the self-pulsing frequency, since one may write the approximate relation $\nu_{\text{self}}=c\ \text{Im}\,\tilde{\lambda}/(2\pi L)$. From our numerical work self-pulsing frequencies in the range of 640 to 670 kHz are found. These numbers agree with the experimental frequency within 10%.

From the above one may conclude that the main experimental facts are predicted correctly by our theoretical description. However, from a detailed comparison it emerges that the agreement between theory and experiment is only qualitative, as numerical discrepancies are found both in the precise position of the instability regions and in the self-pulsing frequency. Whereas theory predicts that the instabilities die out quickly if we leave the bistable range of the upper branch of the stationary curve, the experimental self-pulsing phenomena are still flourishing there. This discrepancy is not removed by adjusting the value of the cooperation parameter somewhat. For instance, the ratios r defined above exactly match if C is chosen to be 266 [2], but this fit does not lead to a substantial extension of the instability interval.

To make a precise check on the self-pulsing frequencies we have computed the theoretical counterpart of Fig. 16 of [2]. In this figure the experimental self-pulsing frequency is plotted as a function of the cavity detuning parameter θ for fixed $\tilde{\Delta}=0.917$ and $\tau_\perp=16.5$. To obtain the theoretical curve we have calculated the imaginary part of the eigenvalue $\tilde{\lambda}$ for the same range of θ-values. In principle, this imaginary part depends on the precise value of $|x|$ within the positive-slope part of the instability domain. However, it turns out that the dependence of Im $\tilde{\lambda}$ on $|x|$ is quite weak, so that it may be neglected here. The experimental and theoretical curves for ν_{self} as a function of θ are given in Fig. 7. Both curves show the same general functional dependence. A quantitative agreement is lacking, however. The theoretical curve does not lie significantly closer to the experimental values than the 'reference" curve [2] that is obtained by employing the rough estimate $\nu_{\text{self}}=c(1+\theta/(2\pi))(2L)^{-1}$.

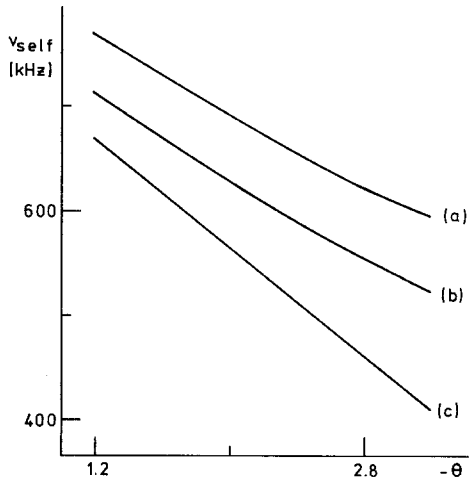

Fig. 7. Self-pulsing frequency ν_{self} as a function of θ for $\tilde{\Delta}=0.917$, $T=0.31$, $C=294$ and $\tau_\perp=16.5$. The label (a) denotes the theoretical curve, (b) the experimental curve and (c) the reference curve

The theoretical results presented above are based on an analysis of the properties of the dispersive instability domain. An extensive numerical search for other instability domains that might be present in the part of parameter space that is explored by the experiments has convinced us that the dispersive instability domain is indeed the only one that needs to be considered here.

In interpreting self-pulsing phenomena for optical bistability in a Fabry-Pérot cavity one has used [2] a so-called equivalent ring cavity of length $2L$ as a model. In an earlier paper [9] we have shown for the special case of absorptive optical bistability that on adopting the ring cavity model one can be led to quite erroneous predictions on the instabilities and the associated self-pulsing, since the stability domains are strongly influenced by standing-wave effects. We are now in a position to check whether this statement remains true for dispersive optical bistability. In I we have already formulated the stability problem for dispersive optical bistability in a ring cavity. By performing a numerical integration of the ensuing differential equations we can determine how the instability domains for the equivalent ring cavity behave upon varying the detuning parameters. Choosing the same parameter values as in the experiments we have found the instability domain presented in Fig. 8. Comparison with Fig. 5 shows that the domain has grown a lot on neglecting the standing-wave effects. In particular, it can be seen that the maximum value of $|x|$ for which instabilities can be present increases by a factor of the order of 4 upon going from the Fabry-Pérot cavity to the equivalent ring cavity. Hence, the adjective 'equivalent' is ill-chosen when it comes to a discussion of instabilities.

In conclusion, we have demonstrated in this paper that a stability analysis of the Maxwell-Bloch equations for a passive medium enclosed in a Fabry-Pérot cavity can explain the findings of the Lille experiment, at least qualitatively. The standing-wave effects occurring in such a cavity have a strong influence on possible instabil-

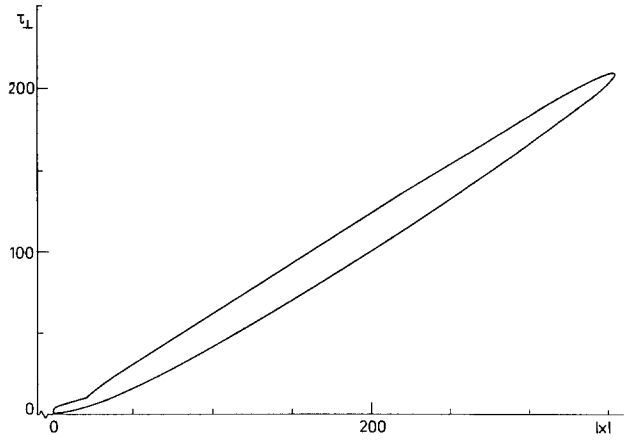

Fig. 8. Instability domain for the nearest side-modes of an equivalent ring cavity. The parameters are the same as in Fig. 5

ities arising in the system, so that the use of a ring cavity model is not justified.

On the basis of a quantitative comparison of theory and experiment it must be admitted, however, that our theoretical results still do not describe the experimental data sufficiently well. Better agreement may arise by slightly adapting some of the parameters in the model. For example, it has not been tested as yet how our results depend on the precise value of the ratio d of the medium damping coefficients. For the absorptive case this dependence has been studied before [9]. Other improvements in the present treatment could come from extensions of the theoretical framework, for instance by including Doppler effects and transverse effects. However, inclusion of the latter effects is particularly important if a plane-wave model overestimates the range of instabilities. In our case the unstable windows along the $|x|$-axis are certainly not too wide.

References

1. van Wonderen, A.J., Suttorp, L.G.: Z. Phys. B – Condensed Matter **83**, 135 (1991)
2. Ségard, B., Macke, B., Lugiato, L.A., Prati, F., Brambilla, M.: Phys. Rev. A **39**, 703 (1989)
3. Ségard, B., Macke, B.: Phys. Rev. Lett. **60**, 412 (1988); Ségard, B., Sergent, W., Macke, B., Abraham, N.B.: Phys. Rev. A **39**, 6029 (1989)
4. Bonifacio, R., Lugiato, L.A.: Lett. Nuovo Cimento **21**, 505, 510 (1978)
5. Hall, G., Watt, J.M. (eds.): Modern numerical methods for ordinary differential equations. Oxford: Clarendon Press 1976
6. Lugiato, L.A.: In: Progress in optics. Wolf, E. (ed.), Vol. XXI, p. 69. Amsterdam: North Holland 1984
7. Casagrande, F., Lugiato, L.A., Asquini, M.L.: Opt. Commun. **32**, 492 (1980); Carmichael, H.J.: Opt. Commun. **53**, 122 (1985); Maize, S., Thompson, B.V., Hassan, S.S.: In: Optical bistability III. Gibbs, H.M., Mandel, P., Peyghambarian, N., Smith, S.D. (eds.), p. 352. Berlin, Heidelberg, New York: Springer 1986; van Wonderen, A.J., Suttorp, L.G.: Physica A **161**, 447 (1989)
8. van Wonderen, A.J., Douwes, B.J., Suttorp, L.G.: Physica A **157**, 907 (1989)
9. van Wonderen, A.J., Suttorp, L.G.: Phys. Rev. A **40**, 7104 (1989); Opt. Commun. **73**, 165 (1989)